Friction
https://doi.org/10.1007/s40544-023-0816-9
ISSN 2223-7690
CN 10-1237/TH
RESEARCH ARTICLE

Experiment and modelling of texture and sliding direction dependence on finger friction behavior

Yuanzhe LI[†], Xue ZHOU[†], Pengpeng BAI, Zhonghuan XIANG, Yonggang MENG, Liran MA[*], Yu TIAN[*]
State Key Laboratory of Tribology in Advanced Equipment, School of Mechanical Engineering, Tsinghua University, Beijing 100084, China
Received: 27 October 2022 / Revised: 06 March 2023 / Accepted: 23 August 2023

Abstract: Humans rely on their fingers to sense and interact with external environment. Understanding the tribological behavior between finger skin and object surface is crucial for various fields, including tactile perception, product appearance design, and electronic skin research. Quantitatively describing finger frictional behavior is always challenging, given the complex structure of the finger. In this study, the texture and sliding direction dependence of finger skin friction was quantified based on explicit mathematic models. The proposed double-layer model of finger skin effectively described the nonlinear elastic response of skin and predicted the scaling-law of effective elastic modulus with contact radius. Additionally, the skin friction model on textured surface considering adhesion and deformation factors was established. It revealed that adhesive term dominated finger friction behavior in daily life, and suggested that object texture size mainly influenced friction-induced vibrations rather than the average friction force. Combined with digital image correlation (DIC) technique, the effect of sliding direction on finger friction was analyzed. It was found that the anisotropy in finger friction was governed by the finger's ratchet pawl structure, which also contributes to enhanced stick-slip vibrations in the distal sliding direction. The proposed friction models can offer valuable insights into the underlying mechanism of skin friction under various operating conditions, and can provide quantitative guidance for effectively encoding friction into haptics.

Keywords: finger friction; tactile perception; tribological model; textured surface; sliding direction

1 Introduction

Tactile perception arises in the process of mechanical contact with the body surface. When human fingers touch and sweep an object surface, contact stress and vibrations are produced, which stimulate cutaneous mechanoreceptors to create tactile images in consciousness. By encoding these tactile signals, information about the object's size, shape, weight, temperature, and material can be perceived by humans. When grasping an object by their fingers, humans can perceive the friction in contact interface and adjust the required force to achieve rapid, accurate, and stable manipulation of various objects, facilitating dexterous interaction between human and the external environment. Accordingly, the mechanical information at the skin–object interface is the essential source of obtaining tactile information, and quantifying the friction interaction at the interface plays a key role in understanding and encoding the tactile information. In order to clarify the correlation between interface friction and tactile perception, research on tactile friction has been increasingly important [1–3], as it can build a bridge between human sensation and tactile surface properties based on the mechanical information of interface friction. Such knowledge is critical in the development of haptic technology [4, 5], functional prostheses [6], and intelligent robotics [7, 8].

[†] Yuanzhe LI and Xue ZHOU contributed equally to this work.
* Corresponding authors: Liran MA, E-mail: maliran@mail.tsinghua.edu.cn; Yu TIAN, E-mail: tianyu@mail.tsinghua.edu.cn

Skin elasticity is one of the dominant parameters affecting friction behavior, and it depends on various factors such as human age [9], gender [10], and skin hydration [11]. In many studies, the mechanical behavior of the skin can be described using Hertz's theory based on the assumption that the material is homogeneous and isotropic with small deformations [12, 13]. The effective elastic modulus E was introduced as an essential parameter to understand the contact and friction behavior of human skin [14, 15]. However, a limitation of this description is that the measured effective elastic modulus exhibits a strong scale dependence, showing a negative correlation with the indenter radius [14]. That is because that skin mainly consists of epidermis, dermis, and subcutaneous tissue, which form a typical multi-layer composite material. The homogeneity assumption is not suitable for such structures, leading to the need for more complex models to accurately describe the mechanical behavior of skin.

Coulomb's law of friction, which assumes a linear relationship between the friction force and the normal force, has been widely used in various contact systems including skin tribology system [16]. However, in the case of skin friction, the relationship between the friction force and the normal force may not be linear due to the complexities in soft contact and surface adhesion. The frictional interaction between skin and an object surface is determined by two main physical factors: An interfacial adhesion term and a deformation resistance term [17, 18]. The adhesion term arises from the adhesion–separation behavior of the actual contact area between the skin and object, while the deformation resistance term arises from the mechanical interaction between the surface asperities [19]. Skin friction is not only determined by the surface properties, but also closely depends on the entire contact system. Factors such as contacting geometry [20], lubricating medium, loading conditions, sliding velocities [21], and supporting stiffness [22] can all have a significant impact on skin friction. One typical example is that in the daily life, human often feel a stronger sensation when sliding their fingers in the distal direction on a textured surface than in the proximal direction, demonstrating an obvious anisotropy of tactile friction. Quantifying the friction behavior for specific contact system was required to fully understand the mechanism of tactile sensation from a tribological perspective.

In this study, texture and sliding direction dependence on finger friction were investigated by utilizing multiple information experiments and quantitative friction models. Specifically, a double-layer elastic model was developed based on the skin structure to investigated skin elasticity and load dependent friction behavior. Interfacial friction between finger skin and textured surface was quantitively investigated from the perspectives of adhesion traction and deformation resistance. In addition, digital image correlation (DIC) technique was utilized to provide *in-situ* skin surface strain information to analyze the effect of sliding direction on finger friction behavior. The results can enhance the understanding of the underlying mechanism of skin friction under different operating conditions, and are expected to provide valuable insights for haptic signals encoding and haptic sensing design.

2 Materials and methods

2.1 Indentation test and measurement of finger contact area

Human finger skin mainly consists of epidermis, dermis, and subcutaneous tissue, which is a typical multi-layer composite material [23], as shown in Fig. 1(a). The average thickness of the epidermis is about 0.2 mm. The stratum corneum, located in the outer layer epidermis, consists of tightly packed keratinocytes, which serves as a crucial barrier for the skin and enhances the hardness of epidermis. It typically has a thickness ranging from 20 to 40 μm. The dermis layer under the epidermis contains various tissues such as touch receptors, nerve fibers, blood vessels, and sweat glands, which are directly related to many functions of human skin. The fat-rich subcutaneous tissue has a thickness of 1–50 mm and functions as mechanical buffering and thermal insulation [14]. Four types of mechanoreceptors in the finger are used to sense the characteristics of touched objects [24], including Merkel's disk (SAI), Meissner's corpuscle (RA1), Pacinian corpuscle (RAII), and Ruffini ending (SAII).

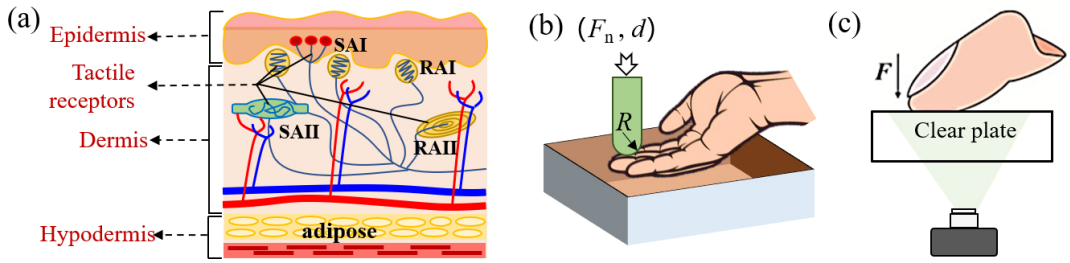

Fig. 1 Schematic illustration of skin structure and elasticity measurement setup. (a) Structure of skin including four mechanoreceptors; (b) schematic of indentation test; and (c) measurement of contact area between finger skin and clear glass plate.

The elasticity is the basic mechanical property of materials, which can remarkably affect the friction of contact systems. The skin elasticity could be measured *in-situ* by performing the indention test, as shown in Fig. 1(b). To control for limited variables in establishing models, only one 26-year-old male participated in all finger friction test voluntarily. He was required to clean the fingers with hand sanitizer and dry it before commencing the test. The comparison of results of more participants of different ages and genders will be considered in our future researches. The universal friction test machine (UMT-5, Bruker) was employed, using a two-dimensional (2D) force sensor (KT500010-1-S) with a measurement range from 0 to10 N and a resolution of 0.5 mN. A steel ball of a diameter 12.6 mm was selected as an indenter to press the index finger of the participant. The normal loads were set between a range from 0 to 0.7 N with an indentation speed of 0.1 mm/s. The indentation depth of skin was calculated from the displacement of indenter subtracting the deformation of cantilever of the force sensor.

To further quantify the skin friction behavior, the contact areas between finger skin and a clear glass plate under different normal loads were recorded by using a high-speed camera (CL600×2/M, Optronis), with a frame rate of 500 fps and a resolution of 1,280 × 1,024 pixels, as shown in Fig. 1(c). The normal loads were recorded by using a 3-axis-force sensor (K3D40, ME-Meßsysteme GmbH) with a measurement range of 10 N. The apparent contact area between the finger and the plate was determined using optical images and analyzed with edge detection and morphological algorithms (more details are shown in Fig. S1 in the Electronic Supplementary Material (ESM)).

2.2 Finger skin friction on textured surface

To investigate the friction behavior of fingers on textured surfaces, we used grid-like textured surfaces with varying interval sizes. It is known that the length scale of a textured surface influences the ability of human to perceive surface roughness [25]. Only for coarse textures with length scales larger than 200 μm, humans can use static force distribution instead of vibration signals to perceive roughness. This force distribution is essentially the elastic contact force. Therefore, we selected relatively coarse textured surfaces with intervals ranging from 0.4 to 1.3 mm. This range was to emphasize the contribution of elastic resistance and to establish a complete friction model while also considering the safety and comfort of the participants. These grid-like surfaces were fabricated on a plate using 3D printing with photosensitive resin. The length and width of the plate were evenly divided into 10 regions for different intervals. A flat surface sample made from the same photosensitive resin was also used as a reference. The surface plate was mounted on a 2D force sensor with a measurement range from 0 to 10 N to measure the sliding friction of the finger under different loads, as shown in Fig. 2. The participant was asked to press the index finger on the sample. The normal load was actively controlled by the participant, varying in

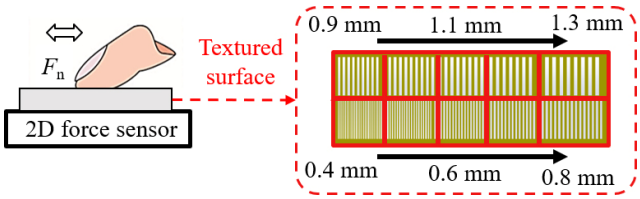

Fig. 2 Schematic of the experimental setup of skin friction on textured surface.

different friction strikes ranging from 1 to 8 N. Unless otherwise specified, the sliding speed of the moving stage (OSMS20-85, SIGMAKOKI) was fixed at 10 mm/s. For velocity varying experiment, it was controlled within the range from 2 to 50 mm/s.

2.3 Bidirectional finger skin friction

To analyze the effect of sliding direction on finger friction behavior, a custom friction setup was used to simultaneously record the friction force and images of contact area, as shown in Fig. 3. The glass plate was fixed on the sample stage, which was installed on a 2D force sensor (K3D40, with a measurement range of 10 N) and a linear moving stage, successively. A binocular camera (LenaCV CAMAR0135-3T16, Wuhan Laina Machine Vision Technology Co., Ltd.) providing stereo vision information was fixed above the sample stage to record the contact area of finger skin, with a frame rate of 90 fps and a resolution of 640 × 480 pixels. The light source was fixed on the same side of cameras. The finger contact area did not change in the image view, which was beneficial for *in-situ* measurement of finger deformation. DIC technology was used to process the image of the finger to obtain the finger surface strain information during the friction process [26, 27] (more details shown in Fig. S2 in the ESM). In this work, the DIC algorithm was achieved based on an open-source software tools in MATLAB platform (The MathWorks Inc., USA) named MultiDIC [28]. The basic procedure of DIC measurement was based on the global matching the features of the speckle pattern through sequence images to reconstruct the surface deformation and strain compared to the initial surface state. The algorithm details can be found in Refs. [28] and [29]. In this test, the participant was asked to keep the index finger contact with glass sample substrate. By fixing the positions of the wrist and hand, the contact angle between the finger and the substrate was controlled to about 25°. Once the position and posture of hand are fixed, the contact angle will have little variation during experiment. The sample stage performed the reciprocated motion at a sliding speed of 10 mm/s. In addition, the water medium was introduced to compare finger friction behavior in the skin dry and wet conditions.

3 Modelling

3.1 Double-layer elastic model of skin

Human skin shows nonlinear and viscoelastic properties. The viscoelasticity was not considered in this study due to the relatively lower contact velocity. Combining the complex properties of finger skin, the mechanical structure of the skin was considered as a double-layer elastic model, including a thin layer with a large elastic modulus (corresponding to the epidermis) and a semi-infinite substrate with a small elastic modulus (corresponding to the subcutaneous tissue). Based on the small deformation assumption, skin mechanical model can be analytically represented by reference to the nanoscale adhesion model proposed by Yang et al. [30], as shown in Fig. 4(a).

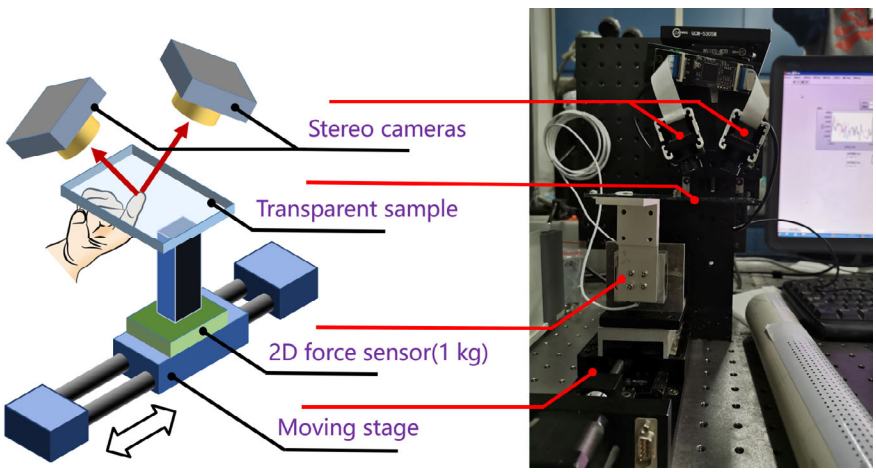

Fig. 3 Bidirectional finger friction setup with stereo camera.

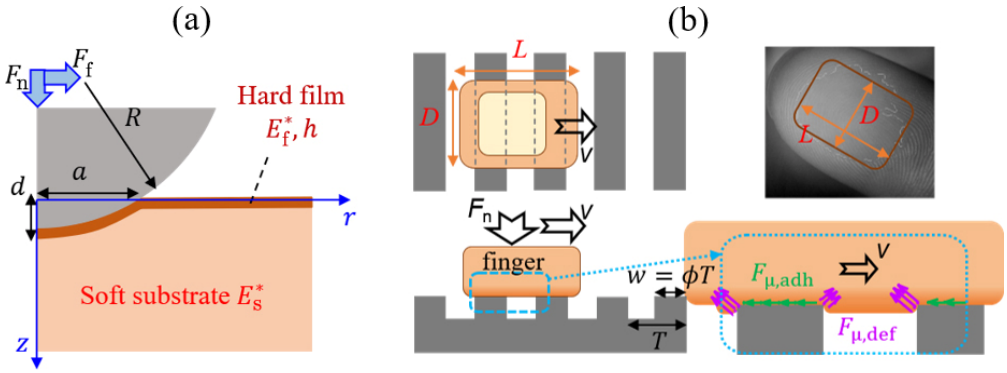

Fig. 4 Schematic of elastic and friction model. (a) Double-layer elastic model of skin and (b) friction model considering the adhesion traction and deformation resistance contribution on textured surface.

The mechanical response function of the indentation depth d applied by a rigid indenter with radius R was set as $F(d)$. It was suggested that the thickness of the thin film layer (marked as f) was much smaller than that of the substrate layer (marked as s), and the elastic modulus was much larger than that of the base, indicating $E_f^* >> E_s^*$. In the indentation test, the mechanical deformation behavior of the relatively hard thin layer was similar to a thin plate. The thin film was mainly affected by tensile and bending deformation, while the substrate was mainly deformed by compression. Considering that a thin hard layer covered on a soft substrate, it was assumed that the stress and deformation state of the substrate was similar to the Hertz contact, and the deformation of the thin layer was consistent with the substrate without thin layer. However, due to the existence of the hard thin film, the force that the double-layer structure required to reach the same indentation depth was greater than the pure soft substrate, indicating that $F = F_s + F_f$, where F_s was the force required for the soft substrate to reach a depth of d. According to the Hertz contact model, it could be expressed as

$$F_s = \frac{4}{3} E_s^* R^{\frac{1}{2}} d^{\frac{3}{2}} \tag{1}$$

where E_s^* was the equivalent elastic modulus, defined as $E_s^* = E_s / (1 - \nu_s)$ with the elastic modulus E_s and the Poisson's ratio ν_s of the substrate.

The additional force F_f caused by the existence of the thin film could be obtained by the mechanical model of the thin plate. Considering that the normal deformation was greater than 1/5 of the thickness of the thin layer, the mechanical equilibrium equation of the thin plate could be calculated by reference of the large deflection equation of the circular thin plate [30]. Assuming that the normal deformation was dominated in the Hertz contact region and the deformation of the contact area was close to the geometric property of the rigid indenter, the term F_f can be expressed as Eq. (2) (more details in the ESM):

$$F_f = \pi E_f^* h \left(\frac{6R^2 d^2 \left(R^2 - Rd\right) - h^2 Rd(4R^2 - Rd)}{6\left(R^2 - Rd\right)^{\frac{5}{2}}} \right) \tag{2}$$

Combining Eqs. (1) and (2), the mechanical response model of the double-layer structure could be deduced. Approximately, it was hypothesized that the thickness h of the layer was very thin compared with R, the higher-order small quantities was neglected in Eq. (2), and the total form of the force was shown as

$$F = F_s + F_f \approx \frac{4}{3} E_s^* R^{\frac{1}{2}} d^{\frac{3}{2}} + \pi E_f^* h R^2 d^2 \left(R^2 - Rd\right)^{-\frac{3}{2}} \tag{3}$$

3.2 Skin friction model based on adhesion and deformation term

In order to explain the skin friction behavior against textured surface, the friction process could be modeled from adhesion and elastic resistance term. The finger skin was simplified as a block elastic body, and its elastic description followed the double-layer structure mechanics model introduced in the previous section. The finger moved at a speed v under the normal load F_n. As a simplification, the apparent contact area

between the finger skin and the plane was considered as a rectangular area with a length of L and a width of D. Then the apparent contact area was $S = LD$. This simplification can be approximated by observing the shape of the contact area between the finger and the glass plate, as shown in Fig. 4(b).

The surface texture width was set as w and the relevant surface ratio defined as $w=\phi T$. Within the range of length L, the number of grids contacted by finger skin was $N=\phi L/w$. For the two basic sources of skin friction [19], the adhesion term ($F_{\mu,\mathrm{adh}}$) was the adhesion between the contact surfaces, which can be calculated from the interfacial shear strength τ and the actual contact area, denoted as $F_{\mu,\mathrm{adh}} = \tau\alpha\left(Dw\right)N$, where α was the ratio of the actual contact area to the apparent contact area. Replacing N with $\phi L/w$ and combining with the relation between load and contact area $S = s_0 F_L^{\lambda}$, the adhesion term could be simplified as

$$F_{\mu,\mathrm{adh}} = \phi\tau\alpha s_0 F_{\mathrm{n}}^{\lambda} \triangleq \phi k_1 F_{\mathrm{n}}^{\lambda} \tag{4}$$

Only when the normal force is sufficiently high that the apparent contact area remains almost unchanged with loading force, k_1 may become load dependent. This situation is outside the scope of our experiments. In this study, k_1 was believed to be an undetermined constant related to the material surface properties.

The deformation term ($F_{\mu,\mathrm{def}}$) was the horizontal component of the elastic resistance from the skin–texture contact, which could be expressed as the product of the static elastic deformation energy U_{def} and the viscoelastic-related dissipation coefficient β. The calculation of elastic deformation was based on the assumption that the contact between a single texture and the skin surface was similar to the contact between a cylinder surface and a plane, and thus the contact force could be expressed as $F_0 = F_{\mathrm{n}}/N \approx (\pi/4)E_{\mathrm{ef}}^{*}D\delta$, where δ was the indentation depth [31]. The corresponding static elastic energy was expressed as

$$U_{0,\mathrm{def}} = \int_0^{\delta} F_0 \mathrm{d}\delta = \frac{\pi}{8}E^{*}D\delta^2 = \frac{2}{\pi}\frac{F_0^2}{E_{\mathrm{ef}}^{*}D} \tag{5}$$

The elastic energy of N texture contacts in all contact areas was $U_{\mathrm{def}} = NU_{0,\mathrm{def}}$. The total elastic energy $U_{x,\mathrm{def}} = U_{\mathrm{def}}x/w$ was produced when the finger moving a distance of x relative to the textured surface. For an ideal elastic contact system, the elastic contact was symmetric in the horizontal direction and the energy was conserved. However, due to the natural viscoelasticity of soft materials such as skin, this part of the stored elastic energy cannot be fully recovered when it was relaxed, and the loss ratio set as β, which made the elastic resistance at the front of the contact to be greater than the elastic recovery force at the back of the contact. The elastic force in the horizontal direction was not zero, providing the deformation resistance term of skin friction:

$$F_{\mu,\mathrm{def}} = \beta\frac{\partial U_{x,\mathrm{def}}}{\partial x} = \frac{2\beta}{\pi\phi s_0 E_{\mathrm{ef}}^{*}}F_{\mathrm{n}}^{2-\lambda} \triangleq \frac{k_2}{\phi}F_{\mathrm{n}}^{2-\lambda} \tag{6}$$

where k_2 was an undetermined constant related to the bulk properties of the material. Combining Eqs. (5) and (6), the total friction coefficient of the textured surface could be obtained:

$$\mathrm{COF} = \frac{F_{\mu,\mathrm{adh}} + F_{\mu,\mathrm{def}}}{F_L} = \phi k_1 F_{\mathrm{n}}^{\lambda-1} + \frac{k_2}{\phi}F_{\mathrm{n}}^{1-\lambda} \tag{7}$$

It could be noted that when the surface ratio of the textured surface was determined, neither k_1 nor k_2 contained the texture dimension term w, meaning that the adhesion term $F_{\mu,\mathrm{adh}}$ of skin friction and the deformation resistance term $F_{\mu,\mathrm{def}}$ were independent of texture size.

Theoretically, both the molecular adhesion term and the deformation resistance term of skin friction can be affected by velocity. For the deformation resistance term, an increase in sliding velocity can lead to a higher energy loss ratio β during a deformation and recovery cycle. For the molecular adhesion term, increasing velocity can have two opposing effects. Higher velocities increase the strength of molecular bonds due to viscoelasticity or more basically thermal activation effect, while higher velocities can also reduce creep effects and reduce the opportunity for molecular adhesion. The interplay between these two opposing effects on friction can both influence the shear stress interfacial shear strength τ, which can be described according to the rate-and-state friction empirical law [32]. Here, we provided a modified form of our friction model considering sliding velocities

dependence as Eq. (8) (more details shown in the ESM):

$$\mathrm{COF}(v)=\phi\left(k_1+qln\left(\frac{v}{v_0}\right)\right)F_{\mathrm{n}}^{\lambda-1}+\frac{k_2v^p}{\phi}F_{\mathrm{n}}^{1-\lambda} \tag{8}$$

Thus, two more parameters p and q (v_0 is a reference velocity) need to be introduced to describe the velocity dependence.

4 Results and discussion

4.1 Finger elastic behavior based on double-layer model

The relation between indentation depth d and normal load F_{n} was shown in Fig. 5(a). The normal force increased with increasing indentation depth, showing an exponential growth. The experimental results were fitted using both Hertz contact model and double-layer model for comparison. The Hertz contact model was only able to fit the upper or lower parts of the data within the range of 2.5 mm indentation depth when using the equivalent elastic modulus E^*= 0.05 MPa, E^*= 0.04 MPa, and E^*= 0.03 MPa. This indicated that the mechanical response of the skin could not be described using a single homogeneous model. However, the experimental data can be well described by the double-layer structure model (Eq. (3)) with a thickness h of 0.2 mm (equivalent to the typical thickness of the skin layer), an elastic modulus E_{f}^* of 0.2 MPa for the hard thin layer, and a E_{s}^* of 0.03 MPa for the soft substrate. These fitting parameters of elastic modulus were found to be comparable to the results obtained by other models [33].

To further verify the model, a high-speed camera was used to simultaneously record the optical image of the finger pressing on the glass surface. The relation between the load force F_{n} and the apparent contact area S were shown in Fig. 5(b). Theoretically, the area–force relation could be also predicted by the double-layer model. Based on the geometric relation of $r=\sqrt{Rd}$ and $S=\pi r^2=\pi Rd$ and the assumption of $R>>d$, the indentation depth d could be replaced by the contact area S in Eq. (3), inducing that

$$F_{\mathrm{n}}=\frac{4}{3}E_{\mathrm{s}}^*\left(\frac{S}{\pi}\right)^{\frac{3}{2}}R^{-1}+\frac{E_{\mathrm{f}}^*}{\pi}hS^2R^{-3} \tag{9}$$

Since the relevant parameters in the skin structure model (i.e., h, E_{f}^*, E_{s}^*) have been independently determined from the previous experiment, the only parameter to be fitted was the equivalent radius of the fingertip R, which was fitted to 15 mm. The fitting results based on the double-layer model was in good agreement with the experimental data, which proved the rationality of the model. In addition, the relation between the contact area S and the external force F_{n} could be expressed as an empirical equation, $S=s_0F_{\mathrm{n}}^{\lambda}$ or $F_{\mathrm{n}}=f_0S^{\frac{1}{\lambda}}$. According to the double-layer elastic model, the contact area in Eq. (4) can be approximated described as $F_{\mathrm{n}}\sim S^{\frac{1}{\lambda}}$. It was readily to see that the value $\frac{1}{\lambda}$ should range from 1.5 to 2, indicating that the value of λ ranged from 0.5 to 0.67. The fitted values in Fig. 5(b) shows that $\frac{1}{s_0}=7\times10^{-5}$, $\lambda=0.52$, which was consistent with the analysis.

The double-layer model can be also used to explain

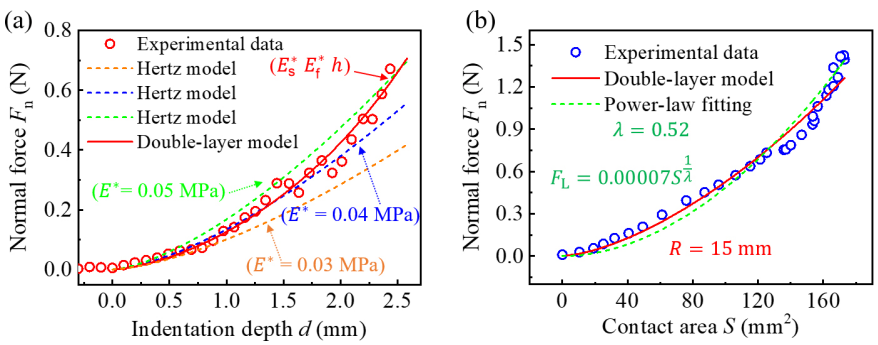

Fig. 5 Elastic behaviors of finger skin during indentation. (a) Relationship between normal force and indentation depth obtained by the indentation test and (b) relationship between normal force and contact area obtained by image processing.

the scale dependence of elastic modulus reported in the literature. Considering the approximation of $R>>d$ (with $R-d\approx R$) and the contact radius $r=\sqrt{Rd}$, Eq. (3) could be simplified as

$$F_{\mathrm{n}}\approx\frac{4}{3}R^{\frac{1}{2}}d^{\frac{3}{2}}\left(E_{\mathrm{s}}^{*}+\frac{3\pi}{4}E_{\mathrm{f}}^{*}hr^{-3}d^{2}\right)\triangleq\frac{4}{3}R^{\frac{1}{2}}d^{\frac{3}{2}}E_{\mathrm{ef}}^{*}(r) \quad (10)$$

Compared to the Hertz model, the effective elastic modulus $E_{\mathrm{ef}}^{*}(r)$ included the contributions of soft substrate and the hard-thin layer. The latter one was a function of the contact radius. The elastic term of the hard-thin layer would be significant for small contact radius, while the effective elastic modulus would converge to the soft substrate elastic term when the contact radius was large. After omitting the constant term, the relationship between elastic modulus and contact scale could be approximately expressed as $E_{\mathrm{ef}}^{*}\sim r^{-3}d^{2}$. In most cross-scale measurements of the skin elastic modulus, ranging from micrometers to millimeters, the indentation depth used was generally similar to the contact radius [14]. Therefore, the above scaling law relation can be simplified as $E_{\mathrm{ef}}^{*}\sim r^{-1}$. The experimental results of the skin elastic modulus at different contact scales, as summarized in Ref. [14], were found to be consistent with the scaling law relation mentioned above.

4.2 Texture dependence of finger friction behavior

Figure 6(a) showed the friction force measured on different textured surfaces as a function of normal load. The smooth surface had a friction force approximately twice that of the textured surfaces when normal force is small, indicating a dependence on contact area. However, although friction force increased with the increase of the load force, a linear fit was not suitable for the entire loading range. It was probably due to the complexities in soft contact and surface adhesion. Despite its nonlinear nature, the friction coefficient could still be used to assess frictional behavior under different normal forces and provide insight into underlying mechanisms, as shown in Fig. 6(b). It was observed that although the friction coefficient decreased with increasing load, there was a significant overlap in the relation between the friction coefficient and load for different textured surfaces, which was consistent with our friction model described by Eq. (7).

The skin friction model on textured surface proposed in this study contained two undetermined parameters: the adhesion parameter k_1 and the deformation resistance parameter k_2. To physically determine the parameters, the adhesion parameter k_1 was obtained from the experimental results measured on a flat surface. In this case, the surface ratio term ϕ equaled 1, and the deformation resistance was assumed to make little contribution. Thus, the friction coefficient can be expressed as $\mathrm{COF}=k_1F_{\mathrm{n}}^{\lambda-1}$, where λ has been independently obtained as 0.52 according to elasticity. Therefore, k_1 could be calculated as 3.6. Subsequently, k_2 was obtained as 0.04 by fitting the friction data on the textured surface with $\phi=0.5$ based on Eq. (7). Theoretical results with independently calibrated parameters showed good agreement with experimental results, as shown in Fig. 6(b), confirming the validity of the proposed model.

The value of λ being smaller than 1 meant that the friction coefficient due to adhesion was negatively

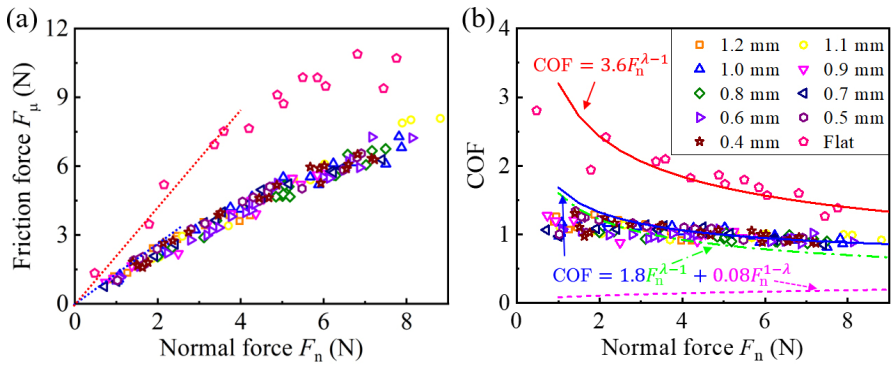

Fig. 6 Finger friction behaviors on textured and flat surfaces. (a) Relationship between friction force and normal load and linear fitting and (b) normal force and friction coefficient and fitting curve based on the friction model.

correlated to the load, while the friction caused by deformation resistance was positively correlated to the load. The negative correlation between friction coefficient and load force suggested that the adhesion played a dominant role in finger rubbing, which was consistent with previous research [18, 34]. Moreover, these two contributions can be quantified. For example, at a load of 5 N, the contribution of adhesion to the total skin friction was about 83%, while the contribution of deformation resistance of the textured surface was about 17%. To find the critical load F_n at which the deformation resistance would contribute half of the friction, we set $F_{\mu,def} = F_{\mu,adh}$ and obtained F_n = 25 N. This force was relatively large for daily finger pressing behavior, and the mechanical response of the skin inner tissue would be exaggerated under this large force, leading to a significantly increased equivalent elastic modulus E^*_{ef} of the human body. Thus, the contribution of deformation resistance predicted by Eq. (7) could be further reduced. Consequently, it could be predicted that the friction behavior of fingers during daily life was predominantly dominated by adhesion, given the lower elastic modulus and larger actual contact area of fingers.

According to the friction model, the friction force was not dependent on the texture size parameter w but only on the surface ratio ϕ. For general random rough surface, the surface ratio can be considered as 0.5, and in this case, friction force may only have a weak relationship with the surface roughness. This was consistent with the conclusion that humans do not perceive surface roughness through averaged friction force but through other attributes such as frictional vibration [14]. Overall, the friction model proposed in this study not only provided a good description of friction experiments on textured surfaces but also effectively quantified the contributions of the two major sources of adhesion and deformation resistance in skin friction.

Our study primarily focused on the scenario of constant sliding velocity. When the sliding velocity changed from 2 to 50 mm/s, there was a slight decrease in friction behavior, as depicted in Fig. S3 in the ESM. The modified model, described by Eq. (8), effectively captured this trend by considering the dominant influence of the adhesion friction term. However, this modified model can only provide a rough estimation of the friction coefficient under steady sliding velocities. Skin friction at high velocities becomes more complex, and unsteady phenomena such as stick–slip may occur. In future studies, more complex dynamic skin friction models will be considered to further understand the velocity dependence.

4.3 Direction dependence of finger friction behavior

The friction between the finger and the glass plate was measured in the direction of sliding back and forth. It was found that the friction force in the distal direction was generally greater than that in the proximal direction both in finger passive sliding conditions (shown in Fig. 7(a)). Upon adding water as a lubricant, the friction between the finger and the glass surface decreased significantly. However, the persistence of friction anisotropy between the distal and proximal directions suggests that the difference in friction is not caused by surface properties. To further clarify it, the relationship between friction coefficient and loading force was summarized in Fig. 7(b). Regardless of

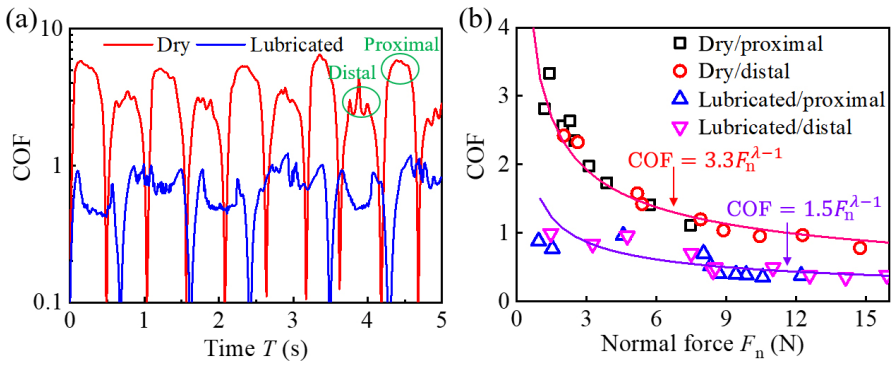

Fig. 7 Direction dependence of finger-skin friction. (a) Friction coefficients during a reciprocating process on flat surface with and without water lubrication and (b) fitting curves based on the friction model.

whether dry contact or water lubrication was used, the relationship between the friction coefficient and load could be described as the form of Eq. (7) with neglecting the deformation resistance term. Furthermore, despite the typically larger normal force in the distal direction than that in the proximal direction, the friction coefficient followed the same curve in both cases. This indicated that the difference in friction between the two sliding directions cannot be attributed to surface anisotropy such as skin ridges, but rather to the difference in normal loading force.

The contact state of the finger and the glass during the proximal and distal sliding could be characterized by the 3D DIC method, which can provide the surface topography and surface stain information *in situ*. For non-contact state, the finger skin showed a slightly curved surface. While for contact state, the surface become relatively flat at the finger–glass interface. Therefore, contact area between finger and the glass plate could be also identified based on the determined position of the glass surface. The experimental results show that the normal force in the distal sliding direction increased and the contact area also increased compared to the static state, showing a large area of compressive strain appearing behind the contact zone (shown in Fig. 8(a)). In the proximal direction, the normal force and contact area were both decreased, showing a relatively small area of compressive strain in front of the contact area.

Based on the observed phenomena and the state of finger contact, the anisotropic friction behavior of fingers can be explained by the physiological structure of fingers, as shown in Fig. 8(b). The state of the tilted finger behaved like a ratchet pawl. For the initial static contact state, the contact angle between finger and surface was set as θ, and the preload normal force F_{n0} was balanced by F_{z0} at finger joint. The structure of the spring (corresponding to the tendon and ligament at the joint, etc.) exerted a constant inner moment M_0 at joint to balance the moment arising from the loading force $M_0 = F_{n0} L\cos\theta$, where L was the knuckle length. In the proximal moving

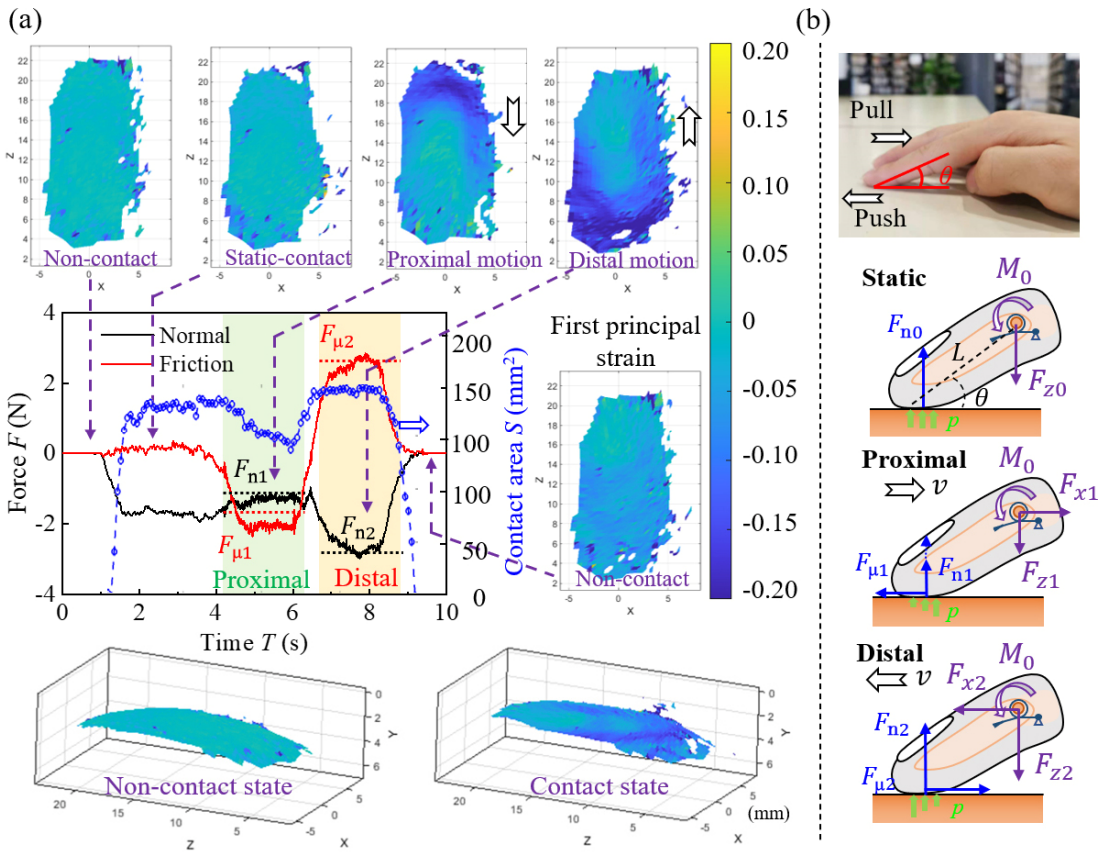

Fig. 8 Finger contact state during the proximal and distal motion. (a) Measurement of contact area and surface train during friction and (b) schematic of pawl-like finger motion model.

direction, the moment of normal force can be cancelled by the friction torque, which decreased the downside normal force. The torque balance takes the form of

$$F_{n1}L\cos\theta + F_{\mu 1}L\sin\theta = M_0 \tag{11}$$

The relationship between friction force and normal force was $F_\mu = 1.5F_n^\lambda$, and λ = 0.52. Thus, the normal force can be expressed as

$$F_{n1} + 1.5F_{n1}^\lambda \tan\theta = F_{n0} \tag{12}$$

While in the distal moving direction, the friction torque and the inner momentum M_0 were coupled to increase the normal force. It can be expressed as

$$F_{n2} - 1.5F_{n2}^\lambda \tan\theta = F_{n0} \tag{13}$$

Knowing the static normal F_{n0} = 1.7 N and the contact angle $\theta \approx 25°$, the normal and tangential forces in the two sliding directions can be calculated as F_{n1} = 1.1 N, $F_{\mu 1}$ = 1.6 N, F_{n2} = 2.8 N, $F_{\mu 2}$ = 2.6 N. These calculated results were marked with dashed lines in Fig. 8(a), which agreed well with measured value. Accordingly, the bidirectional friction difference will decrease within a certain range as the contact angle decreases. However, this anisotropic friction of the finger seems cannot be eliminated due to the fact that the contact angle cannot reach zero, as the supporting joint cannot be positioned on the friction interface.

The phenomenon of anisotropic finger friction was consistent with previous study. Delhaye et al. [35, 36] investigated the surface strain and contact area of the finger and found a difference in skin stiffness for different sliding directions. Camillieri and Bueno [37] observed different finger vibration behavior during sliding and suggested that it could be due to finger biomechanics related to joints, tendons, and muscles. Furthermore, the results of this study suggested that the anisotropic mechanical behavior of the fingertip may influence the perception of roughness [22]. When sliding in the distal or proximal direction, the friction moment can cause an offset in the pressure distribution such that the pressure is greater in the distal direction than in the proximal direction during distal movement. A previous study has shown that the stick–slip phenomenon is more likely to occur in this kind of pressure distribution of the distal sliding direction [38]. The stick–slip induced vibration can match the dynamic response of the Pacinian corpuscle (RAII) [14], leading to a stronger perception of roughness in the distal direction than in the proximal direction.

5 Conclusions

In this study, surface texture and sliding direction dependence of finger skin friction was investigated by both experiments and tribological models. Specifically, a double-layer model, considering a hard-thin layer and a soft substrate, was developed to describe the nonlinear elastic behaviors of the skin, which effectively predicted the force–indentation behavior of skin and the scaling law of skin's effective elastic modulus. Additionally, a friction model for skin on both flat and textured surfaces was developed considering the contributions of adhesion and deformation terms. Based on the independently calibrated parameters, the model exhibited a good fit to the experimental data. It revealed that texture size had little effect on the averaged friction force, and adhesion interaction primarily governed the frictional behavior of the finger in everyday activities. Moreover, combining friction measurement and digital image correlation (DIC) optical measurement technology, the influence of sliding direction on finger friction was analyzed. The provided finger ratchet pawl structure model provided a quantitative explanation for the anisotropic friction behavior, and revealed the presence of enhanced stick–slip vibrations in the distal sliding direction. Overall, this study provides important insights into understanding the complex tribological behaviors in tactile friction processes, and the findings have the potential to guide the development of haptic technologies and inspire advancements in bionic engineering.

Acknowledgements

The authors are grateful for the financial support of the National Natural Science Foundation of China (No. 52175176) and Joint Funds of the National Natural Science Foundation of China (U2141248).

Declaration of competing interest

The authors have no competing interests to declare that are relevant to the content of this article. The author Prof. Yu TIAN is the Editorial Board Member of this journal, and the author Prof. Yonggang MENG is the Associate Editor of this journal.

Electronic Supplementary Material: Supplementary material is available in the online version of this article at https://doi.org/10.1007/s40544-023-0816-9.

References

[1] Meng Y, Xu J, Ma L, Jin Z, Prakash B, Ma T, Wang W. A review of advances in tribology in 2020–2021. *Friction* **10**(10): 1443–1595 (2022)

[2] Zhou X, Masen M A, Mo J, Shi X, He Y, Jin Z. Investigation of experimental devices for finger active and passive tactile friction analysis. *Chin J Mech Eng* **36**(1): 129–139 (2023)

[3] Tang W, Zhang S, Yu C, Zhu H, Chen S, Peng Y. Tactile perception of textile fabrics based on friction and brain activation. *Friction* **11**(7): 1320–1333 (2022)

[4] Huang Y, Yao K, Li J, Li D, Jia H, Liu Y, Yiu C K, Park W Y, Yu X G. Recent advances in multi-mode haptic feedback technologies towards wearable interfaces. *Mater Today Phys* **22**: 100602 (2022)

[5] Choi C, Ma Y, Li X, Chatterjee S, Sequeira S, Friesen R, Felts J R, Hipwell M C. Surface haptic rendering of virtual shapes through change in surface temperature. *Sci Rob* **7**(63): eabl4543 (2022)

[6] Wells E D, Shehata A W, Dawson M R, Carey J P, Hebert J S. Preliminary evaluation of the effect of mechanotactile feedback location on myoelectric prosthesis performance using a sensorized prosthetic hand. *Sensors* **22**(10): 3892 (2022)

[7] Huang J, Zhou J, Wang Z, Law J, Cao H, Li Y, Wang H B, Liu Y H. Modular origami soft robot with the perception of interaction force and body configuration. *Adv Intel Syst* **4**(9): 2200081 (2022)

[8] Hao T, Xiao H, Liu S, Liu Y. Fingerprint-inspired surface texture for the enhanced tip pinch performance of a soft robotic hand in lubricated conditions. *Friction* **11**(7): 1349–1358 (2022)

[9] Gerhardt L C, Lenz A, Spencer N D, Munzer T, Derler S. Skin-textile friction and skin elasticity in young and aged persons. *Skin Res Technol* **15**(3): 288–298 (2009)

[10] Gerhardt L C, Strassle V, Lenz A, Spencer N D, Derler S. Influence of epidermal hydration on the friction of human skin against textiles. *J R Soc Interface* **5**(28): 1317–1328 (2008)

[11] Geerligs M, van Breemen L, Peters G, Ackermans P, Baaijens F, Oomens C. In vitro indentation to determine the mechanical properties of epidermis. *J Biomech* **44**(6): 1176–1181 (2011)

[12] Elleuch K, Elleuch R, Zahouani H. Comparison of elastic and tactile behavior of human skin and elastomeric materials through tribological tests. *Pol Eng Sci* **46**(12): 1715–1720 (2006)

[13] Wang M, Liu S, Xu Z, Qu K, Li M, Chen X, Xue Q, Genin G M, Lu T J, Xu F. Characterizing poroelasticity of biological tissues by spherical indentation: an improved theory for large relaxation. *J Mech Phys Solids* **138**: 103920 (2020)

[14] Van Kuilenburg J, Masen M A, Van der Heide E. Contact modelling of human skin: What value to use for the modulus of elasticity? *Proc Inst Mech Eng Part J* **227**(4): 349–361 (2012)

[15] Crichton M L, Chen X, Huang H, Kendall M A F. Elastic modulus and viscoelastic properties of full thickness skin characterised at micro scales. *Biomaterials* **34**(8): 2087–2097 (2013)

[16] Derler S, Gerhardt L C. Tribology of skin: Review and analysis of experimental results for the friction coefficient of human skin. *Tribol Lett* **45**(1): 1–27 (2011)

[17] Johnson S A, Gorman D M, Adams M J, Briscoe B J. The friction and lubrication of human stratum corneum. In *Thin Films in Tribology, Proceedings of the 19th Leeds-Lyon Symposium on Tribology held at the Institute of Tribology*, Leeds, UK, 1993: 663–672.

[18] Adams M J, Briscoe B J, Johnson S A. Friction and lubrication of human skin. *Tribol Lett* **26**(3): 239–253 (2007)
[19] Fagiani R, Massi F, Chatelet E, Berthier Y, Akay A. Tactile perception by friction induced vibrations. *Tribol Int* **44**(10): 1100–1110 (2011)
[20] Bobjer O, Johansson S E, Piguet S. Friction between hand and handle. Effects of oil and lard on textured and non-textured surfaces; perception of discomfort. *Appl Ergon* **24**(3): 190–202 (1993)
[21] Masen M A, Veijgen N, Klaassen M. Experimental tribology of human skin. In *Skin Biophysics*. Limbert G, Ed. Dordrecht (NLD): Springer, 2019: 281–295.
[22] Zhou X, Mo J L, Li Y Y, Xiang Z Y, Yang D, Masen M A, Jin Z M. Effect of finger sliding direction on tactile perception, friction and dynamics. *Tribol Lett* **68**(3): 85 (2020)
[23] Subramanyan K, Misra M, Mukherjee S, Ananthapadmanabhan K P. Advances in the materials science of skin: A composite structure with multiple functions. *MRS Bulletin* **32**(10): 770–778 (2007)
[24] Kandel E, Schwartz J, Jessel T. *Principles of Neural Science,* 5th Ed. New York (USA): McGraw-Hil, 2013.
[25] Hollins M, Bensmaïa S J. The coding of roughness. *Can J Exp Psychol* **61**(3): 184–195 (2007)
[26] Li Y, Bai P, Cao H, Li L, Li X, Hou X, Fang J B, Li J Y, Meng Y G, Ma L R, Tian Y. Imaging dynamic three-dimensional traction stresses. *Sci Adv* **8**(11): eabm0984 (2022)
[27] Pan B, Qian K, Xie H, Asundi A. Two-dimensional digital image correlation for in-plane displacement and strain measurement: A review. *Meas Sci Technol* **20**(6): 062001 (2009)
[28] Solav D, Moerman K M, Jaeger A M, Genovese K, Herr H M. MultiDIC: An open-source toolbox for multi-view 3D digital image correlation. *IEEE Access* **6**(pp): 30520–30535 (2018)
[29] Blaber J, Adair B, Antoniou A. Ncorr: Open-source 2D digital image correlation matlab software. *Exp Mech* **55**(6): 1105–1122 (2015)
[30] Yang F K, Zhang W, Han Y, Yoffe S, Cho Y, Zhao B. "Contact" of nanoscale stiff films. *Langmuir* **28**(25): 9562–9572 (2012)
[31] Knothe K. *Contact Mechanics and Friction Physical Principles and Applications*. Dordrecht (NLD): Springer, 2011.
[32] Rice J R, Ruina A L. Stability of steady frictional slipping. *J Appl Mech* **50**(2): 343–349 (1983)
[33] Tang W, Liu R, Shi Y, Hu C, Bai S, Zhu H. From finger friction to brain activation: Tactile perception of the roughness of gratings. *J Adv Res* **21**: 129–139 (2020)
[34] Leyva-Mendivil M F, Lengiewicz J, Page A, Bressloff N W, Limbert G. Skin microstructure is a key contributor to its friction behaviour. *Tribol Lett* **65**(1): 12 (2017)
[35] Delhaye B, Lefevre P, Thonnard J L. Dynamics of fingertip contact during the onset of tangential slip. *J R Soc Interface* **11**(100): 20140698 (2014)
[36] Delhaye B, Barrea A, Edin B B, Lefevre P, Thonnard J L. Surface strain measurements of fingertip skin under shearing. *J R Soc Interface* **13**(115): 20150874 (2016)
[37] Camillieri B, Bueno M A. Influence of finger movement direction and fingerprints orientation on friction and induced vibrations with textile fabrics. *Tribol Lett* **69**(143): 1–17 (2021)
[38] Tian P, Tao D, Yin W, Zhang X, Meng Y, Tian Y. Creep to inertia dominated stick–slip behavior in sliding friction modulated by tilted non-uniform loading. *Sci Rep* **6**: 33730 (2016)

Yuanzhe LI. He received his B.S. degree in mechanical engineering from Xi'an Jiaotong Univiersity in 2017 and Ph.D. degree in mechanical engineering at Tsinghua University in 2022. His research interests include tactile friction, surface forces, and nanothermal engineering.

Xue ZHOU. She received her B.S. and Ph.D degrees in mechanical engineering from Southwest Jiaotong University in 2016 and 2022, received general engineering diploma from École Centrale de Lyon, France, in 2016. She is now following a postdoctoral period at the State Key Laboratory of Tribology in Advanced Equipment (SKLT), Tsinghua University. Her research interests include biotribology, bionic tribology, and tactile friction.

Pengpeng BAI. He received his Ph.D. degree at China University of Petroleum (Beijing), in 2017, majoring in materials science and engineering. Following a postdoctoral period at SKLT in Tsinghua University, he is now working as an associate researcher in the Department of Mechanical Engineering, Tsinghua University. He has published over 40 papers. His research interests include the interface science and technology, high temperature liquid lubricant, and corrosion protection mechanism of metals, etc.

Zhonghuan XIANG. He received his B.S. degree in mechanical engineering from Tsinghua University. Now he is a Ph.D. candidate in the Department of Mechanical Engineering, Tsinghua University, China. His current research focuses on tactile friction.

Yonggang MENG. He received his M.S. and Ph.D. degrees in mechanical engineering from Kumamoto University, Japan, in 1986 and 1989, respectively. He joined the SKLT at Tsinghua University in 1990. His current position is a professor, and his research areas cover the tribology of micro-electromechanical systems (MEMS) and hard disk drives, active control of friction and interfacial phenomena, and nanomanufacturing.

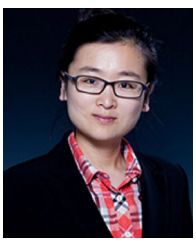

Liran MA. She received her B.S. degree from Tsinghua University in 2005, and received her Ph.D. degree from Tsinghua University in 2010. Following a postdoctoral period at the Weizmann Institute of Science in Israel, she is now working as an associate professor in the SKLT, Tsinghua University. Her interests in tribology have ranged from aqueous lubrication and hydration lubrication to the liquid/solid interface properties. She has published over 50 papers. Her honors include the Hinwin Doctoral Dissertation Award (2011), the Maple Leaf Award for Outstanding Young Tribologists (2015), and Chang Jiang Scholars Program-Young Professor Award (2015).

Yu TIAN. He is a professor and director of the SKLT at Tsinghua University of China. He gained his B.S. and Ph.D. degrees in mechanical engineering at Tsinghua University in 1998 and 2002, respectively. Subsequently, he joined the SKLT. He was a postdoc at the University of California, Santa Barbara with professor Jacob ISRAELACHVILI from 2005 to 2007. His research interest is the science and technology at the interface of physics, materials, engineering, and biology to understand the physical laws of adhesion, friction, and rheology to implement technological inventions to benefit the society. He has received the Youth Science and Technology Award of China (2016), the Yangtze River Scholars Distinguished Professor (2015–2019), the National Natural Science Foundation for Distinguished Young Scientists of China (2014), the Wen Shizhu-Maple Award-Young Scholar Award (2012), the Young Scholar Achievement Award of the Society of Mechanical Engineering of China (2011), Outstanding Young Scholar Award of the Chinese Tribology Institute (2009), and the National Excellent Doctoral Dissertation of China (2004).